Systematic and Applied Microbiology 49 (2026) 126730

Contents lists available at ScienceDirect

Systematic and Applied Microbiology

journal homepage: www.elsevier.com/locate/syapm

Gelidimonas denitrificans gen. nov., sp. nov., and *Gelidimonas diazotrophica* sp. nov. psychrophilic bacteria involved in the nitrogen cycle in tundra soils of South Spitsbergen

Jakub Grzesiak [a], Julia Brzykcy [a,b], Peter Young [c], Elvira Krakowska [d], Robert Stasiuk [b], Kamil Krakowski [e], Przemysław Decewicz [f], Alina Kiedryńska [d], Renata Matlakowska [b,1], Dariusz Bartosik [d,*,1]

[a] Department of Antarctic Biology, Institute of Biochemistry and Biophysics, Polish Academy of Sciences, Pawinskiego 5A, 02-106 Warsaw, Poland
[b] University of Warsaw, Faculty of Biology, Institute of Microbiology, Department of Geomicrobiology, Miecznikowa 1, 02-096 Warsaw, Poland
[c] Department of Biology, University of York, York YO10 5DD, United Kingdom
[d] University of Warsaw, Faculty of Biology, Institute of Microbiology, Department of Bacterial Genetics, Miecznikowa 1, 02-096 Warsaw, Poland
[e] University of Warsaw, Faculty of Biology, Institute of Evolutionary Biology, Laboratory of Structural Bioinformatics, Zwirki i Wigury 101, 02-089 Warsaw, Poland
[f] University of Warsaw, Faculty of Biology, Institute of Bioengineering, Laboratory of Applied Microbial Ecology, Miecznikowa 1, 02-096 Warsaw, Poland

ARTICLE INFO

Keywords:
Gelidimonas
Oxalobacteraceae
Psychrophilic bacteria
Denitrification
Nitrogen fixation
Ornithogenic soil
Arctic environment

ABSTRACT

Two Gram-negative, psychrophilic, denitrifying bacterial strains, D2 and D11, were isolated from ornithogenic soil collected at a breeding colony of the marine bird *Alle alle* on Spitsbergen Island, Svalbard (Norway; High Arctic). Complete genome sequencing revealed that each strain possesses a single circular chromosome (3.83 Mbp and 3.63 Mbp, respectively) with similar GC content (55.3% and 55.5%), as well as plasmids – one shared by both strains (26.3 kb) and one unique to strain D11 (16.3 kb). Despite their striking genetic similarity, the two strains exhibit distinct physiological characteristics. Strain D2 is a facultative chemolithoautotroph capable of using hydrogen as an energy source and assimilating carbon dioxide and dinitrogen, whereas strain D11 displays a strictly heterotrophic lifestyle. Although the 16S rRNA genes of D2 and D11 share a high level of sequence identity (99.6%), whole-genome comparative analyses, including digital DNA–DNA hybridization (dDDH) and average nucleotide identity (ANI), indicated that they represent two distinct species within the family *Oxalobacteraceae* (class *Betaproteobacteria*). Core proteome-based phylogenetic analysis of *Oxalobacteraceae* unambiguously placed both strains within the family; however, neither clustered with any currently described genus. We therefore propose that these strains represent a novel genus, *Gelidimonas* gen. nov., with type species *Gelidimonas denitrificans* sp. nov. (type strain D11^T) and a second species *Gelidimonas diazotrophica* sp. nov. (type strain D2^T).

Introduction

Despite the harsh environmental conditions, polar regions are inhabited by metabolically diverse microorganisms (Malard and Pearce, 2018). This microbial diversity underlies a wide array of metabolic traits and biochemical processes that play a crucial role in shaping biogeochemical cycles. There is growing concern about the impact of climate change on polar biota and the potential acceleration of microbial activity (Ernakovich et al., 2022; Descamps et al., 2017; Schuur et al., 2022). These concerns arise from thawing permafrost, increased nutrient availability and altered organic matter input. Together, these factors stimulate microbial metabolism, leading to significant changes in carbon and nitrogen cycling. The polar microbiota not only plays a major role in the transformation of local environments, but also has a broader global impact, as its activity can lead to increased greenhouse gas (GHG) emissions, contributing to the ongoing climate crisis.

Of particular concern is nitrous oxide (N_2O), a greenhouse gas primarily of microbial origin, with denitrifying bacteria being its main

* Corresponding author.
E-mail address: d.bartosik@uw.edu.pl (D. Bartosik).
[1] †equal contribution

https://doi.org/10.1016/j.syapm.2026.126730
Received 23 December 2025; Received in revised form 7 May 2026; Accepted 11 May 2026
Available online 14 May 2026

natural source – responsible for approximately 70% of its global emissions (Mosier, 1998). Since N_2O is also a significant factor in stratospheric ozone depletion, recognizing and characterizing its natural sources is essential. In our previous study, we conducted microbiological and geochemical analyses of soil samples collected on Spitsbergen Island (Norway; High Arctic) to evaluate the N_2O emission potential of these soils. The results revealed that ornithogenic soil from a breeding colony of the marine, planktivorous bird species *Alle alle* (little auk) is likely the most potent source of N_2O in this region (Brzykcy et al., 2026). Two bacterial strains, D2 and D11, isolated from this environment and classified within the family *Oxalobacteraceae* (order: *Burkholderiales*, class: *Betaproteobacteria*, phylum: *Pseudomonadota*), were the subject of investigation in the present study.

There are currently 29 validly published names of genera in the *Oxalobacteraceae*: *Actimicrobium*, *Affinundibacterium*, *Cognatundibacterium*, *Collimonas*, *Duganella*, *Glaciimonas*, *Herbaspirillum*, *Herminiimonas*, *Janthinobacterium*, *Keguizhuia*, *Lacisediminimonas*, *Massilia*, *Mokoshia*, *Naxibacter*, *Neoundibacterium*, *Noviherbaspirillum*, *Oxalicibacterium*, *Oxalobacter*, *Paraherbaspirillum*, *Parundibacterium*, *Paucimonas*, *Pseudoduganella*, *Pseudundibacterium*, *Rugamonas*, *Sapientia*, *Solimicrobium*, *Telluria*, *Undibacterium* and *Zemynaea* (https://lpsn.dsmz.de/family/oxalobacteraceae). The family was originally defined by its ability to degrade oxalate in animal intestines, first observed in *Oxalobacter formigenes* (Allison et al., 1985).

Representatives of the family *Oxalobacteraceae* are widely distributed and have been isolated from diverse habitats, including soil, freshwater environments (such as rivers, lakes, and groundwater), plant materials, animal intestines, sewage, and even desert ecosystems. They exhibit substantial metabolic diversity and a broad range of phenotypic traits and ecological adaptations. Most members are mesophilic heterotrophs, although some have developed adaptations to psychrophilic conditions (Baldani et al., 2014). The family also shows considerable variation in oxygen requirements – most species are aerobic or microaerophilic, while members of the genus *Oxalobacter* are obligate anaerobes (Baldani et al., 2014; Ma et al., 2023). Motility is common among members of this family, typically mediated by one or more polar flagella, although some species are nonmotile (e.g. *Oxalobacter formigenes*, *Glaciimonas immobilis* and *Glaciimonas singularis)* (Baldani et al., 2014).

The aim of the present study was to perform physiological, genomic and phylogenetic characterization of the two isolated strains D2 and D11, and to determine their evolutionary relationships.

Materials and methods

Sampling site and strain isolation

Ornithogenic soil (OS) samples were collected from areas influenced by a little auk (*Alle alle*) colony located near The Stanisław Siedlecki Polish Polar Station in Hornsund, Spitsbergen Island (Svalbard Archipelago, High Arctic) (77°00′33.3" N 15°31′49.1″ E). Samples were collected in replicates ($n = 4$) from a depth of 5–10 cm. The replicates were pooled, divided into sub-samples, and immediately frozen at −20 °C until further processing. Microbial cells were extracted as follows: 1 g of soil was mixed with 20 mL of 0.9% (w/v) NaCl and 10 mM tetrasodium pyrophosphate ($Na_4P_2O_7$) solution and shaken at 1000 rpm for 30 min at 4 °C. Then the sample was sonicated in a 4 °C water bath for 5 min, vortexed and centrifuged at 129 rcf for 1 min. The sediment was discarded, and the supernatant, containing a suspension of cells, was used for bacterial cultivation targeting psychrophilic denitrifiers. The procedure was adapted from Elliott and Des Jardin (1999), Grzesiak et al. (2020) and Lunau et al. (2005).

Serial dilutions of cell suspension (10^0 to 10^{-5}) were spread on plates with a modified R3A medium for denitrifiers (R3D), which included (g L^{-1} final conc.): KNO_3 – 5 g L^{-1}, R3D base Tryptone – 1 g L^{-1}, Peptone – 1 g L^{-1}, Yeast extract – 1 g L^{-1}, Beef extract – 1 g L^{-1}, $MgSO_4$ x $7H_2O$ – 0.1 g L^{-1}, NORIT® activated charcoal – 0.2 g L^{-1}, bacteriological agar – 15 g L^{-1}), phosphate buffer (K_2HPO_4 – 1 g L^{-1}, NaH_2PO_4 – 0.5 g L^{-1}), carbon source mix (1 g L^{-1} each; Glycerol, Na-Acetate, Na-Lactate, Na-Pyruvate, Na-Citrate, Methanol, Ethanol) and 1 mL L^{-1} of SL-11 trace element solution (Atlas, 2010). KNO_3 solution, phosphate buffer, carbon sources and SL-11 trace element solution were filter-sterilized and added to autoclaved R3D base. Plates were incubated anoxically at 5 °C in the dark for 6 weeks using GENbag ANAER generators (bioMèrieux, Marcy l'Etoile, France). Colonies were tested for gas production using Durham tubes in 20 mL of liquid R3D medium under the same conditions. Gas-producing strains were maintained oxically in R2A medium at 5 °C.

Provisional strain identification was based on 16S rRNA gene sequence similarity. DNA was extracted by boiling in a 5% Chelex-100 solution. The rRNA genes were amplified using standard primers (27f/1492r) and sequenced as previously described (Grzesiak et al., 2020). Sequences were compared with validly named species in EzBioCloud (Chalita et al., 2024) and NCBI reference RNA sequences database (refseq_rna) database. The strains were deposited in the public BCCM/LMG Bacteria Collection and DSMZ - German Collection of Microorganisms and Cell Cultures GmbH under the numbers: $D2^T$ = $LMG34059^T$ = $DSM120165^T$ and $D11^T$ = $LMG34060^T$ = $DSM\ 120166^T$.

Colony/cellular morphology and phenotype assessment

To observe colony morphology, strains were grown on R2A solid medium, for 2 weeks at 10 °C. For cell morphology analysis, the strains were grown in R2A liquid medium on a rotary shaker at 120 rpm for 96 h. Cell morphology and ultrastructure were analyzed using scanning electron microscopy (SEM; CrossBeam 540 Zeiss, Oberkochen, Germany) and transmission electron microscopy (TEM; TALOS F200X, Thermo Fisher Scientific, Waltham, MA, USA), respectively. The presence of flagella was tested using TEM following negative staining with 2.0% uranyl acetate and placement on a carbon-coated copper grid.

Enzyme activity, carbon source utilization, and chemical sensitivity of bacterial cultures were evaluated using API ZYM, API 20NE (bioMérieux, Marcy l'Etoile, France), and BIOLOG GEN III MicroPlates (Biolog, Hayward, CA, USA) tests. All tests were conducted at 10 °C over a two-week incubation period, with evaluations performed weekly. Oxidase activity was determined using oxidase test sticks (Bactident Oxidase, Merck), and catalase activity was tested by adding 3% hydrogen peroxide to the culture and observing bubble formation within 10 min. Growth characteristics were monitored on Luria-Bertani (LB), Nutrient broth (NB), Trypticase Soya Broth (TSB) and R2A media. Anaerobic growth was evaluated on R2A medium using GENbag ANAER (bioMérieux, Marcy l'Étoile, France).

Bacterial growth under different temperature, pH and salinity conditions was evaluated using R2A liquid medium in three biological replicates. Bacterial cultures were diluted to an initial optical density (OD) of 0.05 at wavelength of 600 nm and dispensed to microtiter plates (200 µL) in at least three technical replicates. The plates were incubated statically under appropriate temperatures (10 °C for bacterial growth estimation under different pH values and salinity) for 96 h. Absorbance values were measured at 600 nm every 24 h using a Tecan Sunrise absorbance microplate reader (Tecan, Männedorf, Switzerland).

Growth was assessed at seven temperatures (0, 5, 10, 15, 20, 25, and 30 °C). For the 0 °C condition, rejuvenated bacterial culture was transferred to PCR tubes and incubated in a thermocycler. Bacterial growth at different pH levels (4.0–9.0) was tested in R2A liquid medium buffered with MES, PIPES, HEPES, or TRIS buffers, each at a final concentration of 0.05 M. The medium was divided into four aliquots, each supplemented with one buffer, and the pH was adjusted using 5 M H_2SO_4 or NaOH to values within the buffer's effective range: 4.0–6.0 for MES, 6.5–7.0 for PIPES, 7.5–8.0 for HEPES, and 8.5–9.0 for TRIS. After reaching one target pH, a portion was set aside, and the rest was adjusted to the second value. Buffered media were sterilized by autoclaving and dispensed into microtiter plates for growth assays. NaCl

effects on bacterial growth were evaluated in R2A liquid medium supplemented with varying concentrations of NaCl to simulate different salinity levels. The final tested NaCl concentrations were 0%, 0.5%, 1%, 2%, 3%, 4%, 5%, 6%, 7% and 8% (w/v) respectively. NaCl was thoroughly dissolved in the medium before sterilization by autoclaving, and the prepared media were then distributed into microtiter plates for growth testing. Denitrification was assessed by monitoring gas accumulation in Durham tubes in R3D medium. The ability of bacteria to grow chemolithoautotrophically using CO_2 as the sole carbon source and H_2 as the sole electron source was tested using Basal Mineral Medium for Cultivating Hydrogen-Oxidizing Bacteria according to the procedure described by Aragno and Schlegel (1992) (the cultures were maintained at 10 °C for 3 weeks).

Whole-cell fatty acid composition

Cultures of D2 and D11 strains were grown in liquid R2A medium at 10 °C on a rotary shaker at 120 rpm until approximately 80 mg of biomass was obtained for each strain. Fatty acid methyl esters (FAMEs) were extracted according to the protocol of Sasser (2006) in three replicates for each strain. Fatty acids identification was performed using a gas chromatograph 7890 A (Agilent Technologies, Santa Clara, CA, USA) equipped with a mass spectrometer (MS 5975c, Agilent Technologies, Santa Clara, CA, USA). Samples were injected (inlet temp 250 °C, split mode ratio of 1:5) into the DB-WAX column (L × ID 30 m × 0.250 mm, average thickness 15 μm, Agilent Technologies, Santa Clara, CA, USA). Separation employed a seven-step temperature program: (i) 100 °C for 8 min, (ii) increase to 130 °C at 7 °C/min, hold 1 min, (iii) increase to 135 °C at 1 °C/min, (iv) decrease to 130 °C at 20 °C/min, hold 5 min, (v) increase to 135 °C at 1 °C/min, hold 2 min, (vi) increase to 160 °C at 4 °C/min, (vii) increase to 230 °C at 20 °C/min, hold 2 min. The Mass Selective Detector (MSD) operated at 70 electronvolts (eV) in dual scan/selected ion monitoring (SIM) mode. The source temperature was 230 °C, and the quadrupole temperature was 150 °C. The full scan ranged from *m/z* 50–550, whilst SIM mode targeted the molecular ion and other appropriate ions selected from the fragmentation pattern, each ion having a dwell time of 100 milliseconds. Bacterial Acid Methyl Esters standard (BAME, Supelco, Bellefonte, USA) was used for identification and calibration (Fig. S2AB).

Nitrogen fixation-acetylene reduction assay (ARA)

Cultures of D2 and D11 strains were preincubated in liquid R2A medium at 10 °C on a rotary shaker at 120 rpm. Two-weeks-old cultures were centrifuged and washed twice with 0.9% (w/v) NaCl solution. The acetylene reduction assay was performed in 100 mL serum bottles sealed with butyl rubber stoppers and aluminium caps. Each bottle was filled with 50 mL of diazotrophic medium (RBA) (DSMZ medium 441). Three replicates per strain and four controls were prepared. Then, 5 mL of headspace gas was replaced with 5 mL of acetylene (10% vol). Cultures were incubated at 10 °C in the dark. Acetylene and ethylene concentrations were monitored during incubation. Headspace samples (5 mL) were collected using a gas-tight syringe and analyzed by gas chromatography (GC 7890 A, Agilent Technologies, Santa Clara, CA, USA) coupled with flame ionization detector (FID, Agilent Technologies, Santa Clara, CA, USA). The injector and detector temperatures were 100 °C and 280 °C, respectively. Carrier gas flow rates were 45 mL/min for nitrogen, 450 mL/min for air, and 40 mL/min for hydrogen. A sample was injected with a split ratio of 1:10 into the HP-PLOT-Q column (L × ID 30 m × 0.320 mm, average thickness 20 μm, Agilent Technologies, Santa Clara, CA, USA). The temperature was held at 40 °C for 12 min. Final measurements were taken after 30 days.

Genome sequencing and consequent analyses

Genomic DNA was extracted using Genomic Mini AX Bacteria (A&A Biotechnology, Poland) and quantified fluorometrically with the PicoGreen reagent (Life Technologies, Carlsbad, USA) on an Infinite Tecan platform. Two sequencing platforms were used: Illumina (short reads) and Oxford Nanopore (long reads). For Illumina sequencing, DNA was fragmented using Covaris E210, libraries were prepared with the NEBNext® Ultra™ II DNA Library Prep Kit (New England Biolabs, Ipswich, USA), and sequencing was performed on a MiSeq system in paired-end mode (300 cycles). Nanopore libraries were prepared using the Rapid Barcoding Kit (SQK-RBK004) and sequenced on a MinION device with a Flongle R10.4.1 flow cell. Genome assembly was performed analogously to the methods described in Korsak et al. (2025). Short and long reads were filtered with fastp (v0.24.0) and fastplong (v0.2.1) (Chen, 2023), respectively. Each read type was filtered in two ways depending on its downstream application: light filtering for genome assembly and more stringent filtering for polishing. Residual adapter sequences in Nanopore reads were removed with Porechop_ABI (v0.5.0) (Bonenfant et al., 2022). A total of 12 assemblies were generated using multiple assemblers, including Flye (2.9.5) (Kolmogorov et al., 2019), miniasm (v0.3) and Minipolish (v0.1.2), (Wick and Holt, 2021), as well as Raven (v1.8.3) (Vaser and Šikić, 2021). The resulting assemblies were subsequently clustered to generate a consensus assembly using Trycycler (v0.5.6) (Wick et al., 2021). The consensus assembly was polished with Medaka (v2.1.1) (Nanopore Technologies, 2025). Additional polishing was performed using Pilon (v1.24) (Walker et al., 2014) with short reads, both before and after genome rotation to *dnaA* (chromosomes) or *rep* (plasmids) using Dnaapler (v1.3.0) (Bouras et al., 2024). Final polishing was carried out with Polypolish (v0.6.1) (Wick and Holt, 2022). Short-read mapping for polishing was performed using BWA-MEM2 (v2.2.1) (Vasimuddin et al., 2019). Final genome annotation was performed using Bakta (v1.11.4) (Schwengers et al., 2021), and genome completeness was assessed with BUSCO (v6.0.0) (Manni et al., 2021) using the burkholderiales_odb10 dataset.

Metagenomic sequencing

Metagenomic DNA was extracted from the OS sample, from which the D2 and D11 strains were originally isolated, as well as from the microcosm (ORP) – an OS incubated at 10 °C for 100 days under anaerobic conditions on R3A medium supplemented with glucose as carbon source (1 g L^{-1}) and nitrates (5 g L^{-1}), to enrich the native denitrifying bacterial populations. DNA was extracted in triplicate from 0.25 g of crude soil/soil microcosm using the DNeasy PowerSoil Kit (QIAGEN, Hilden, Germany) following the manufacturer's instructions. The triplicate DNA extracts were then pooled prior to sequencing.

Metagenomic DNA was sonicated using a Covaris S220 to generate fragments of approximately 500 bp, and purified using Kapa Pure Beads (Roche, Basel, Switzerland) at a 1:1 sample-to-reagent volume ratio. Libraries were constructed using the KAPA Hyper Prep Kit (Roche) and TruSeq DNA UD Indexes (Illumina), followed by six cycles of enrichment PCR. DNA fragments of approximately 650 bp were selected using Kapa Pure Beads (Roche) using a two-step purification (sample-to-reagent volume ratio: 1:0.55 and 1:0.65, respectively). Library fragment sizes were assessed using a TapeStation 2200 with High Sensitivity D1000 reagents (Agilent, Santa Clara, USA), and concentrations were determined by qPCR using the Kapa Library Quantification Kit (Kapa Biosciences, Wilmington, USA). DNA sequencing was performed on an Illumina NovaSeq 6000 platform using the NovaSeq 6000 SP Reagent Kit v 1.5 (500 cycles) in paired-end 2 × 250 cycle read mode, following the manufacturer's standard protocol and including a 1% PhiX control library (Illumina).

Bioinformatic analyses

Homology searches were conducted using BLASTN and BLASTP tools available on the NCBI website, with default settings (Altschul et al., 1997), and the HHpred server (Söding et al., 2005). Comparative

genomic analyses were conducted with Proksee (Grant et al., 2023). Prophage sequences were predicted using PHASTEST (PHAge Search Tool with Enhanced Sequence Translation) (Wishart et al., 2023), accessed through the Proksee platform (https://proksee.ca/). The search for CRISPR-Cas systems was performed using CRISPRCasFinder (Couvin et al., 2018). Insertion sequences (IS) were identified and classified through comparative sequence analysis using the ISfinder database (Siguier et al., 2006). A search for integrative and conjugative/mobilizable elements was performed using ICEfinder 3.0 (Wang et al., 2024). Biosynthetic gene clusters were identified using antiSMASH (bacterial version) (Medema et al., 2011). Whole genome taxonomy was performed using the Type (Strain) Genome Server (TYGS) (Meier-Kolthoff and Göker, 2019) and Genome Taxonomy Database Toolkit (GTDB-Tk) (Parks et al., 2020). Average Nucleotide Identity (ANI) and Average Amino Acid Identity (AAI) values were calculated based on the genomic sequences of *Oxalobacteraceae* reference strains obtained from the GenBank database. ANI was computed using pyANI-plus v1.0.0 (Pritchard et al., 2016) with the dnadiff method for all compared genomes and, additionally, the anib method for D2 and D11 strains. Furthermore, ANI and ANIb values for strains D2 and D11 were independently calculated using the JSpecies Web Server (JSpeciesWS) (Richter et al., 2015). AAI was calculated using EzAAI v1.2.4 (Kim et al., 2021) with default settings. For AAI, values were additionally weighted by the fraction of homologous proteins shared between each genome pair to account for differences in proteome coverage. Heatmaps of ANI and AAI were generated by converting similarity values to distances (using the formula 100 – AAI) and performing hierarchical clustering with Ward's method, using pandas v1.4.3 (McKinney, 2010), Matplotlib v3.4.3 (Hunter, 2007), and SciPy v1.7.3 (Virtanen et al., 2020) in Python v3.9.19.

The presence of D2 and D11-related species in the metagenomic datasets was investigated by mapping two Illumina metagenomics read datasets (OS and ORP) against their genomes. Raw reads were first filtered using fastp v0.23.4 (Chen et al., 2018) in paired-end mode and then aligned with bwa-mem v2.2.1 (Vasimuddin et al., 2019) using default settings. The resulting mapping files were processed with coverM v1.36 (Aroney et al., 2025) to determine sequencing depth, relative abundance, and the fraction of the genome covered in each metagenomic dataset. Additionally, the mapping files were analyzed using pysam v0.23.3 (Li et al., 2009; Bonfield et al., 2021; Danecek et al., 2021) and pycirlize v1.10.1 [https://github.com/moshi4/pyCirclize] (python packages in Python v3.9.19) to generate coverage plots. Coverage was calculated using a 500-bp sliding window.

Core proteome analysis

Pairwise similarity between genomes was represented by the core proteome amino acid identity index (cpAAI) calculated from the 375 core proteins of the *Oxalobacteraceae* using the R script provided by Florent Lassalle at https://github.com/flass/cpAAI_Rhizobiaceae (Kuzmanović et al., 2021).

A core proteome phylogeny was constructed using the 375 core proteins of the *Oxalobacteraceae* that were identified by Ma et al. (2023). The 375 proteins from *Collimonas antrihumi* DSM 104040^T were used as queries in a BLASTP search to identify the orthologous sequences in the predicted proteomes of all genomes of type strains of species in the *Oxalobacteraceae* available at NCBI, as well as in D11, D2 and the other genomes identified as potential members of the new genus. Duplicate genomes were discarded, as well as those in which fewer than 90% of the core proteins could be identified, except that the five *Oxalobacter* spp. genomes were retained despite lacking about 50 of the proteins. Of the 191 genomes in the final phylogeny, 177 had at least 370 of the 375 proteins. Protein sequences were aligned using Clustal Omega 1.2.3 (Sievers et al., 2011). A maximum likelihood phylogeny was constructed from the concatenated sequences using IQ-TREE 2.3.4 (Minh et al., 2020) using the ModelFinder option (Kalyaanamoorthy et al., 2017) to select the optimal substitution model (LG + F + I + G4). Branch support was assessed using both SH-like aLRT and ultrafast bootstrap (1000 replicates each).

To identify the *Gelidimonas*-specific proteins, all proteins predicted to be encoded by the genome of D11 (the type strain of the type species of the new genus) were used as queries in a BLASTP search of all genomes of type strains in the family *Oxalobacteraceae*. Hits with a score of at least 100 and a percent identity of at least 50% were recorded as evidence of the presence of that protein in that type strain. Proteins were considered specific to *Gelidimonas* if present in the nine high-quality *Gelidimonas* genome assemblies (the tenth, cluster3_bin.239, GCA_039931835.1, was excluded because it has a CheckM completeness of only 63%) but absent in all other genomes.

Results and discussion

Geomicrobiological background

The two bacterial strains, D2 and D11, were isolated from ornithogenic soil affected by little auks. The general geochemical and microbiological characteristics of the studied soil were described by Brzykcy et al. (2026). Field-measured soil temperature and pH were 7.63 ± 0.28 °C and 6.52 ± 0.25, respectively. Soil water content and soil organic matter content were 41.00 ± 2.1% and 9.90 ± 0.009%, respectively. The average total carbon, nitrogen and sulfur concentration were 170 g kg^{-1} dm (dry mass), 48 g kg^{-1} dm, and 35.3 g kg^{-1} dm, respectively. Organic carbon amounts in the examined soil were 23.7 g kg^{-1} dm. The concentration of nitrates was estimated at 1.3 mg kg^{-1} dm.

The microbial cell abundance in the studied soil was 7.39 × 10^{10} cells g^{-1} dm. *Pseudomonadota* and *Acidobacteriota* were the most abundant bacterial phyla, with relative abundance of 33% and 19%, respectively. The relative abundance of bacteria belonging to the class *Betaproteobacteria*, order *Burkholderiales* and family *Oxalobacteraceae* were 8.28%, 1.87%, and 0.55%, respectively (Brzykcy et al., 2026).

Phenotypic characteristics of D2 and D11 strains

The isolation of bacterial strains was directed towards psychrophilic denitrifiers. To this end, a nitrate-containing medium was used under anaerobic conditions at 5 °C. The D2 and D11 strains were capable of utilizing nitrate as an electron acceptor, as confirmed by the API 20 NE test. Furthermore, their denitrification activity and gas production in nitrate-amended medium were confirmed. Both strains grew on R2A medium and were characterized as facultatively anaerobic, Gram-stain-negative, rod-shaped bacteria that are motile by means of polar flagella (Fig. 1ABCD). Cells were approximately 0.5–0.8 μm in diameter and 1.8–3.2 μm in length (Fig. 1AB) and accumulated polyhydroxyalkanoate (PHA) granules (Fig. 1EF). These bacteria formed circular, white colonies (0.3–1 mm in diameter) after two weeks of incubation on R2A agar medium at 10 °C. Both strains were catalase and oxidase negative.

The D2 and D11 strains were psychrophilic, with an optimum growth temperature of 10 °C. No growth was observed below 5 °C or above 20 °C (D2) and 15 °C (D11). The pH range for growth was 5.5 to 8.0, with optimum growth at pH 6.0–6.5 (D2) and 6.5–7.0 (D11). Neither strain required NaCl for growth but both tolerated up to 3% (w/v) NaCl. All data pertaining to the growth analyses are provided in Fig. S1.

Both strains showed growth under aerobic and anaerobic conditions on Nutrient Agar; additionally, strain D11, in contrast to D2, was also capable of growth on nutrient-rich LB medium and Trypticase Soya Broth. Biochemical characterization of the strains was performed using API ZYM, API 20NE and Biolog GEN III systems. In the API ZYM, strain D2 showed positive activity for alkaline phosphatase, valine arylamidase, α-chymotrypsin, leucine arylamidase, acid phosphatase, and naphthol-AS-BI-phosphohydrolase. In the API 20 NE, it tested positive for nitrate reduction, assimilation of malic acid, trisodium citrate and potassium gluconate. Respiration-based analysis using the Biolog system

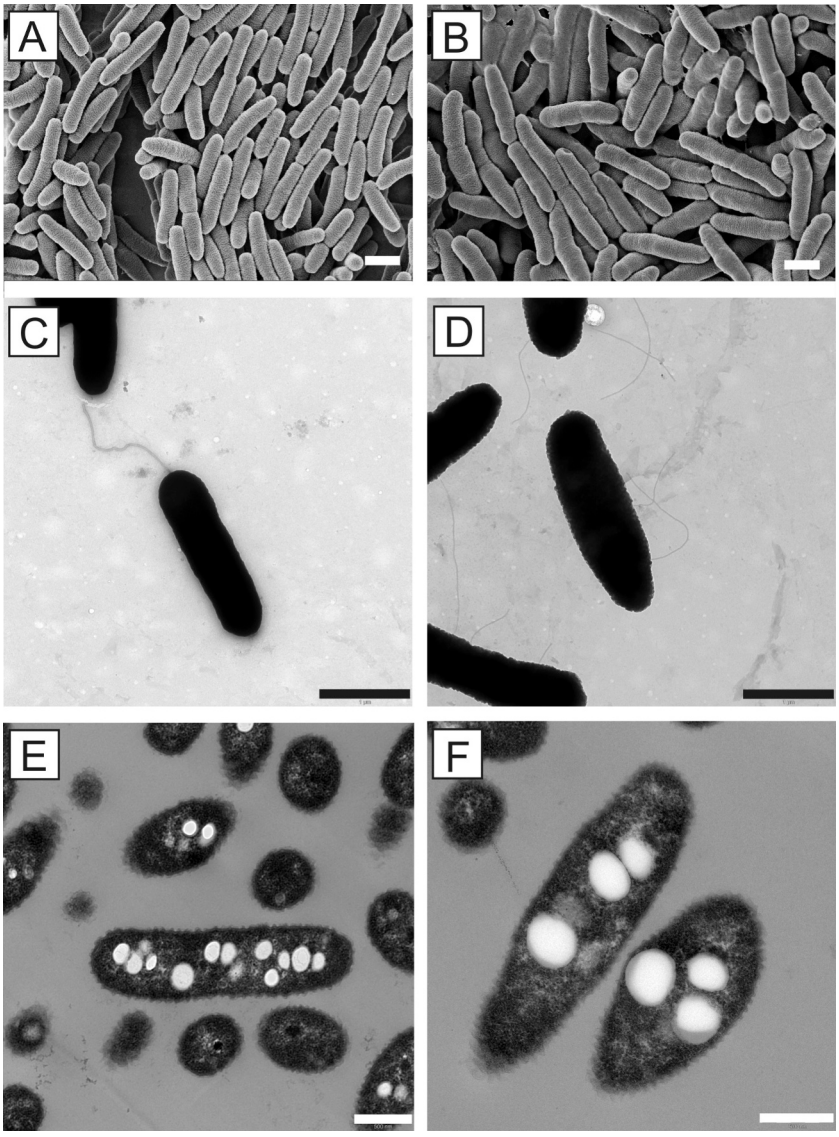

Fig. 1. Electron micrographs of cells of D2 (A, C, E) and D11 (B, D, F) strains grown on R2A medium at 10 °C. A, B – scanning electron micrographs; bar 1 μm. C, D – transmission electron micrographs of cells that were negatively stained with uranyl acetate; bar – 1 μm; E, F – transmission electron micrographs of ultrathin sections; bar – 500 nm.

GEN III indicated that the strains were able to metabolize only a limited number of organic substrates. Surprisingly, they were unable to use carbohydrates as sole carbon sources. Strain D2 was capable of oxidizing the following carbon sources: acetic acid, bromo-succinic acid, citric acid, D-aspartic acid, D-malic acid, L-malic acid, propionic acid, sodium lactate 1%, α-keto-butyric acid, β-hydroxy-D,L-butyric acid, γ-amino-butyric acid and D-serine. In the antibiotic sensitivity assay D2 was negative for rifamycin SV and lincomycin.

Strain D11 showed positive activity for leucine arylamidase, acid phosphatase, and naphthol-AS-BI-phosphohydrolase (API ZYM). In the API 20 NE, it tested positive for nitrate reduction, assimilation of malic acid, production of indole and esculin hydrolysis. D11 was capable of oxidizing acetic acid, citric acid, D-malic acid, L-malic acid, propionic acid, sodium lactate 1%, α-keto-butyric acid, β-hydroxy-D,L-butyric acid and γ-amino-butyric acid (Biolog GEN III). The antibiotic sensitivity assay was negative for lincomycin. All data pertaining to the biochemical analyses are provided in Table S1.

The major cellular fatty acids for both strains were unsaturated cis-9-hexadecenoic acid (C16:1 ω7c) and saturated hexadecanoic acid (C16:0) (Table 1) (chromatograms are shown in Fig. S2). The average content of C16:1 ω7c in strains D2 and D11 was 75.69% and 83.99%, respectively, while C16:0 accounted for 7.99% and 10.52%. Additionally, unsaturated trans-9-octadecenoic acid (C18:1 ω9t) was detected in D2, with an average content of 9.92% (Table 1).

General genomic properties

The complete nucleotide genomic sequences of the D2 and D11 strains revealed that both contain single circular chromosomes, with sizes of 3,829,060 bp (D2) and 3,631,096 bp (D11), and similar GC content of 55.3% and 55.5%, respectively (GenBank accession numbers: CM146349.1 and CM146350.1, respectively). In addition, the strains harbor extrachromosomal replicons: D2 carries plasmid pD2_1 (26,349 bp) (GenBank: JBSYGK010000002.1), while D11 carries two plasmids – pD11_1 (26,352 bp), sharing 99.98% overall sequence identity with pD2_1, and pD11_2 (16,319 bp) GenBank: JBSYGS010000002.1 and JBSYGS010000003.1, respectively). The chromosomes contained 3451 (D2) or 3268 (D11) coding sequences, 4 rRNA loci and 56 (D2) or 57 (D11) tRNA genes. A summary of genomic features is provided in Table 2.

Table 1
Comparison of the fatty acid (FA) contents (%) of D2 and D11 isolates. – not detected; TR-traces (<0.1%).

FA (%)	D2	D11
Saturated		
C11:0	TR	TR
C12:0	0.15	3.03
C13:0	–	TR
C14:0	0.45	1.42
C15:0	–	0.10
C16:0	7.99	10.52
C19:0	TR	TR
Unsaturated		
C16:1 ω7c	75.69	83.99
C18:1 ω9c	1.95	–
C18:1 ω9t	9.92	0.68
C20:1 ω11c	TR	TR
Hydroxy		
C12:0 3-OH	1.05	–
C14:0 2-OH	TR	TR
Branched-chain		
iC15:0	TR	TR
iC16:0	TR	TR
iC17:0	TR	TR
aC15:0	TR	–

Table 2
Genomic features of the D2 and D11 strains.

Property	D2 strain (chromosome/plasmid 1)	D11 strain (chromosome/plasmid 1/plasmid 2)
Genome size (bp)	3,829,060/26,349	3,631,096/26,352/16,319
GC content (%)	55.3/52.2	55.5/52.2/54.4
Topology	C/C	C/C/C
No. plasmids	1	2
CDS (chromosome)	3451	3268
Pseudogenes	2	3
rRNA loci	4	4
tmRNA genes	1	1
tRNA genes	56	57
ncRNA genes	7	8

The chromosomes of these strains exhibit synteny and a significant level of sequence conservation. Structural variations are primarily limited to insertions and deletions of DNA fragments of variable lengths, with only a few instances of inversions or translocations (Fig. S3). The D2 and D11 chromosomes share 2736 genes; however, each strain contains a substantial number of unique genes – 738 in D2 and 574 in D11 (Table S2).

According to RAST annotation both genomes contained 293 subsystems, with a low overall subsystem coverage of 27%. The major subsystems included amino acids and derivatives (286/269 genes in D2/D11), carbohydrates (179/153 genes), protein metabolism (155/157), cofactors, vitamins, prosthetic groups, and pigments (153/138), and respiration (113/80). Genes involved in elemental metabolism included those associated with nitrogen (89/57), phosphorus (20/21), potassium (6/6), sulfur (5/3), and iron (4/3). Additionally, a substantial number of genes were related to stress response (64/45) as well as motility and chemotaxis (22/16), reflecting the strains' capacity to adapt to challenging environmental conditions.

antiSMASH analysis predicted that both strains are likely to produce ectoine (with high confidence) – an osmolyte that functions as a stress and thermal protectant (Ng et al., 2023) – and non-ribosomal peptides (type I NRPS, with lower confidence). The obtained results also suggest the potential for the synthesis of arylpolyene (APE), terpenes (and their precursors), and ribosomally synthesized and post-translationally modified peptides (RiPP-like). Additionally, the D2 strain contains a redox cofactor protocluster. No clustered regularly interspaced short palindromic repeats (CRISPRs) or CRISPR-associated genes were detected in either genome (CRISPRFinder).

Both genomes also lack integrated prophages (PHASTEST), but each strain carries a distinct set of transposable elements (TEs). D2 encodes transposases belonging to the Tn*3*, IS*As1*, IS*3*, IS*5*, IS*200*/IS*605* and IS*1182* families, and D11 encodes transposases typical for the IS*3*, IS*30*, IS*66*, IS*110*, IS*200*/IS*605* and IS*256* families (ISfinder). In addition, D11 carries a Tn*7*-family transposon (25,492 bp) integrated in the terminal part of a gene encoding AAA+ family ATPase. This element encodes components of type III restriction and modification (RM) system and numerous hypothetical proteins of unknown function. Similar elements were not detected in GenBank sequences (BLASTN).

Predicted core and strain-specific metabolic properties

The D2 and D11 strains encode the same core metabolic pathways. Both harbor genes for complete glycolysis (the Embden-Meyerhof-Parnas pathway)/gluconeogenesis, pyruvate oxidation, tricarboxylic acid (TCA), and pentose phosphate pathways (PPP). The strains also contain genes for the glyoxylate cycle, allowing utilization of two-carbon compounds, and the methylcitrate cycle, which plays an essential role in propionate metabolism (Clark and Cronan, 2005). They also carry complete genetic information for the catabolic β-oxidation pathway, with multiple genes encoding enoyl-CoA hydratases and 3-ketoacyl-CoA thiolases, indicating the important role of fatty acids metabolism in these bacteria.

Both strains also contain the full set of genes required for biosynthesis of various enzyme cofactors and vitamins, including thiamine, riboflavin, NAD, coenzyme A, pimeloyl-ACP, biotin, lipoic acid, tetrahydrofolate, molybdenum cofactor, PreQ1, siroheme, heme, cobalamin and ubiquinone, which are essential for numerous key metabolic processes.

The genomes encode numerous transporter proteins, most of unknown substrate specificity. Among the well-conserved are putative carriers for amino acids, C4-dicarboxylates, dipeptides, D-glutamate, benzoate, and tricarboxylates – compounds that can serve as carbon and energy sources. Notably, the genomes lack phosphotransferase system (PTS) genes that mediate uptake of carbohydrates, which is consistent with their inability to utilize the tested sugar substrates for growth.

In silico analysis revealed that D2 and D11 strains harbor several genes potentially involved in biosynthesis and degradation of poly-3-hydroxybutyrate (PHB). The main gene cluster encodes PhbF, a transcriptional repressor that regulates expression of genes involved in PHB metabolism (Kadowaki et al., 2011), along with PhbB (acetoacetyl-CoA reductase) and PhbC (polyhydroxyalkanoic acid synthase). In addition, both strains encode PhbA (acetyl-CoA acyltransferase) as well as three poly PHB/PHA depolymerases, and D(−)-3-hydroxybutyrate oligomer hydrolase, enabling complete degradation of PHB into monomers that can enter metabolic pathways.

Furthermore, both strains possess complete high-affinity phosphate-specific transport (Pst) systems. Genes associated with inorganic phosphate storage were also identified, including those encoding polyphosphate kinase (Ppk), responsible for polyphosphate (poly-P) synthesis, and exopolyphosphatase (Ppx), which catalyzes poly-P degradation (Rao et al., 2009). These findings suggest that the strains are capable of storing phosphorus in the form of high-energy polyphosphate granules, which may serve as an energy and phosphate reservoir under nutrient-limited conditions.

D2 and D11 also harbor a complete set of genes involved in denitrification, confirming the results of the phenotypic analyses. They encode (i) respiratory nitrate reductase complex that reduces nitrate (NO_3^-) to nitrite (NO_2^-), consisting of the catalytic subunit NarG and accessory subunits NarH, NarI and NarJ, (ii) cytochrome *cd*1-type nitrite reductase (NirS), which catalyzes the reduction of nitrite NO_2^- to nitric oxide (NO), (iii) a nitric oxide reductase complex, responsible for reduction of NO to nitrous oxide (N_2O), composed of the catalytic

subunit NorB and accessory proteins NorC, NorQ, NorD and NorE, and (iv) a nitrous oxide reductase complex that reduces N_2O to dinitrogen (N_2), consisting of NosZ enzyme and accessory proteins NosF, NosY, NosD, NosR and NosL (Zumft, 1997; Jones et al., 2008). Interestingly, in strain D2 the *nor* gene cluster is duplicated, which could potentially enhance the kinetics of nitric oxide reduction and thereby affect the dynamics of denitrification.

In addition to denitrification, the nitrogen metabolism of both strains includes the nitrate assimilation pathway, enabling the uptake of nitrate and its subsequent reduction to ammonium (NH_4^+), which may then be incorporated into organic compounds such as amino acids. The clustered genes responsible for this pathway encode an assimilatory nitrate reductase, subunits of assimilatory nitrite reductase (NirB, NirD), the nitrate transporter of the major facilitator superfamily, components of nitrate ABC transport system, as well as serine/threonine kinase and the regulatory protein NasT, which is presumed to modulate the expression of the reductase genes (Nie et al., 2024).

Both strains carry a complete set of genes required for the biogenesis, assembly, and regulation of a functional flagellum. The flagellar gene clusters are directly associated with chemotaxis genes CheY, CheB, CheD, CheR (Hazelbauer et al., 2008), indicating tight coordination between motility and environmental sensing. Additionally, D2 encodes YcgR, a *c*-di-GMP-responsive flagellar brake protein, suggesting a potential regulatory mechanism for motility in response to intracellular signaling. These strains also harbor genes typical for the type IV mannose-sensitive hemagglutinin (MSHA) pilus system. MSHA pili, as described in *Vibrio cholerae* (Floyd et al., 2020), are likely critical for beneficial attachment of bacterial cells to abiotic surfaces and biofilm formation.

Interestingly, despite striking genetic similarities between the D2 and D11 strains, the former contains several unique gene clusters that likely determine its distinct metabolic properties. These include the complete Calvin-Benson-Bassham (CBB) cycle with ribulose-1,5-bisphosphate carboxylase/oxygenase (RuBisCO), which enables autotrophic carbon dioxide (CO_2) fixation and its conversion into organic biomass (Meloni et al., 2023). The strain also carries genes involved in hydrogen (H_2) sensing and metabolism, encoding [NiFe] hydrogenases (HoxA, HoxB/HupU, HoxC/HupV, HoxX), Hyp proteins (HypCDEF, HypB) for active site assembly and nickel incorporation, the NAD-reducing [NiFe] hydrogenase complex (HoxFUYH) with maturation factor HoxW, and the uptake hydrogenase (HyaA) for hydrogen oxidation. These enzymes have potential to catalyze the oxidation of molecular hydrogen (H_2), thereby enabling bacteria to harness H_2 as an energy source (Greening et al., 2016). Furthermore, D2 contains a cluster of genes encoding a molybdenum type nitrogenase (NIF), an enzyme crucial for nitrogen fixation (Fig. 2). The NIF cluster also encodes all proteins necessary for nitrogenase synthesis and activity, including those involved in molybdenum uptake, cofactor biosynthesis ([Fe—S] cluster assembly), and the formation of an electron transfer complex required for the nitrogenase function (Edgren and Nordlund, 2004). The activity of nitrogenase in D2 was experimentally validated using the acetylene reduction assay (ARA) (Fig. S4). In addition, the D2 strain was able to grow on nitrogen-free minimal medium. Together, these results demonstrate that this gene cluster confers the full capacity for nitrogen fixation to the host organism.

Taken together, the above data indicate that the D2 strain is a facultative chemolithoautotrophic bacterium capable of using hydrogen as an energy source as well as assimilating CO_2 and N_2. The nitrogenase, RuBisCO and hydrogenase proteins of D2 show the highest amino acid sequence similarities to those found in different *Betaproteobacteria*, particularly members of the family *Oxalobacteraceae*. Intriguingly, the D2 NIF cluster is flanked on one side by an IS*5*-family insertion sequence (Fig. 2). A similar genetic arrangement has been observed e.g. in the chromosomes of *Herbaspirillum seropedicae* SmR1 and *Burkholderia vietnamiensis* G4 (Pedrosa et al., 2011), suggesting that transposable elements may facilitate the horizontal spread of NIF clusters. Strain D11, despite the overall genetic similarities, lacks the genes required for chemolithoautotrophy and displays a heterotrophic lifestyle. We confirmed experimentally the ability of strain D2 to grow chemolithoautotrophically using CO_2 as the sole carbon source and H_2 as the sole electron source. Strain D11 did not grow under these conditions.

Adaptation to cold environments

D2 and D11 strains harbor similar genetic determinants involved in adaptation to cold environments. These include genes encoding protein chaperones, members of the Cold Shock Protein (CSP) family (presumptive RNA chaperons), and genes involved in the synthesis of cryoprotectants and terpenoids.

Both strains carry genes potentially involved in trehalose biosynthesis – a disaccharide that plays a protective role against osmotic stress, desiccation, and freezing (Kuczyńska-Wiśnik et al., 2024). Instead of the most common pathway, which converts UDP-glucose and glucose-6-phosphate into trehalose, they encode two alternative biosynthesis routes: (i) the TreY–TreZ pathway (maltooligosyltrehalose synthase and maltooligosyltrehalose trehalohydrolase), in which the substrates (oligomaltodextrins or glycogen) are converted to trehalose via maltooligosyltrehalose intermediates, and (ii) the TreS pathway, involving trehalose synthase, which reversibly converts maltose into trehalose through a single transglycosylation reaction. The genes of both pathways are located in the proximity of genes involved in the synthesis of glycogen (glycogen synthase GlgA and branching enzyme GlgB), which primarily serves as an energy reserve. The metabolism of these two carbohydrates is interconnected, with enzymes capable of interconverting glycogen to trehalose, thereby facilitating the mobilization of the stored carbon reserve for metabolic needs or stress protection (Pan et al., 2008).

The strains also contain three genes encoding key enzymes involved in the isoprenoid biosynthesis pathway: (i) squalene synthase, which produces a precursor of hopanoids (terpenoids that serve as functional analogs of sterols in bacterial membranes), (ii) phytoene synthase, which catalyzes the formation of a precursor for carotenoid biosynthesis, and (iii) squalene/phytoene desaturase (HopC), which participates in the production of hopanoids or carotenoid derivatives. These compounds enhance membrane stability and protect cells from oxidative and thermal stress.

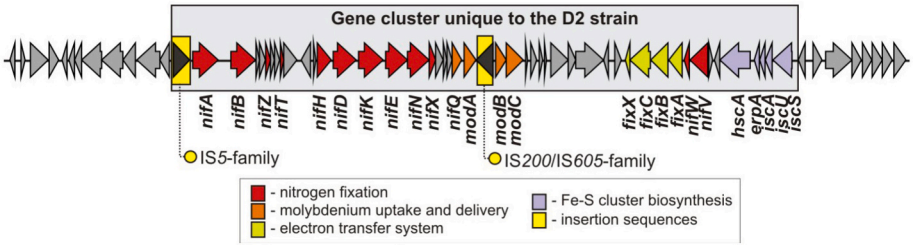

Fig. 2. Genetic organization of the nitrogenase gene cluster (NIF) of the D2 strain.

D2 and D11 represent a novel taxonomic genus

The 16S rRNA gene sequences of D2 and D11 strains (GenBank: PX735051 and PX735050, respectively) share 99.6% sequence identity, which, according to established guidelines (≥98.5%; Stackebrandt and Ebers, 2006), suggest that they might belong to the same species. However, genome-scale comparative analysis, including Digital DNA-DNA Hybridization (dDDH) and Average Nucleotide Identity (ANI), did not support this classification. The dDDH value was 67.4% (using formula d_0 [Auch et al., 2010]; 95% confidence interval: 63.5–71.0) and the ANI/ANIb values were 94.3%/94.1% (94.36/93.90 when calculated using JSpeciesWS) (Fig. 3), whereas the generally accepted thresholds for species delineation are 70% and 95%, respectively. These values, being slightly below these cutoffs, indicate that the analyzed strains represent distinct but closely related species.

Comparative analysis of D2 and D11 16S rRNA gene sequences (BLASTN) against reference RNA sequences database (refseq_rna; NCBI) revealed the highest sequence identity to *Herminiimonas saxobsidens* NS11 (D2: 97.54%, D11: 97.3%) and several other members of the genus *Herminiimonas* (family *Oxalobacteraceae*), with a minimum sequence identity of 96.99% to *Herminiimonas arsenicoxydans* ULPAs1 (NR_125502.1). A similar analysis performed using the EzBioCloud 16S database showed the highest sequence similarity to *Herminiimonas contaminans* CCUG 53591 (D2: 97.64%, D11: 97.85%) with a minimum sequence identity of 96.97% to *H. arsenicoxydans* ULPAs1. The analysis revealed also significant, but lower, sequence identity to other (non-*Herminiimonas*) members of the family, ranging from 95.7% to 96.6%.

The strains analyzed in this study represent a clear example demonstrating that drawing taxonomic conclusions solely on the basis of 16S rRNA gene sequence similarity can be misleading. The commonly accepted thresholds for the identification of novel species and genera are ≥98.5% and 94.5% 16S rRNA gene sequence identity, respectively (Stackebrandt and Ebers, 2006; Yarza et al., 2014). According to these criteria, strains D2 and D11 might be classified within the same species (99.6% identity), and their sequence similarity to representatives of other genera within the family *Oxalobacteraceae* (e.g., *Herminiimonas* spp., approximately 96–98%) would not justify their assignment to a novel genus. However, the recent summary by Hackmann (2025) indicates that, in 90% of all cases, sequences from the same species share a minimum of 97.2–100% identity, while intergeneric values range from 90.1% to 99.0%, demonstrating that there are numerous exceptions to these generally accepted rules. This study highlights the critical importance and necessity of inferring bacterial phylogeny based on comprehensive core genome analyses encompassing higher taxonomic

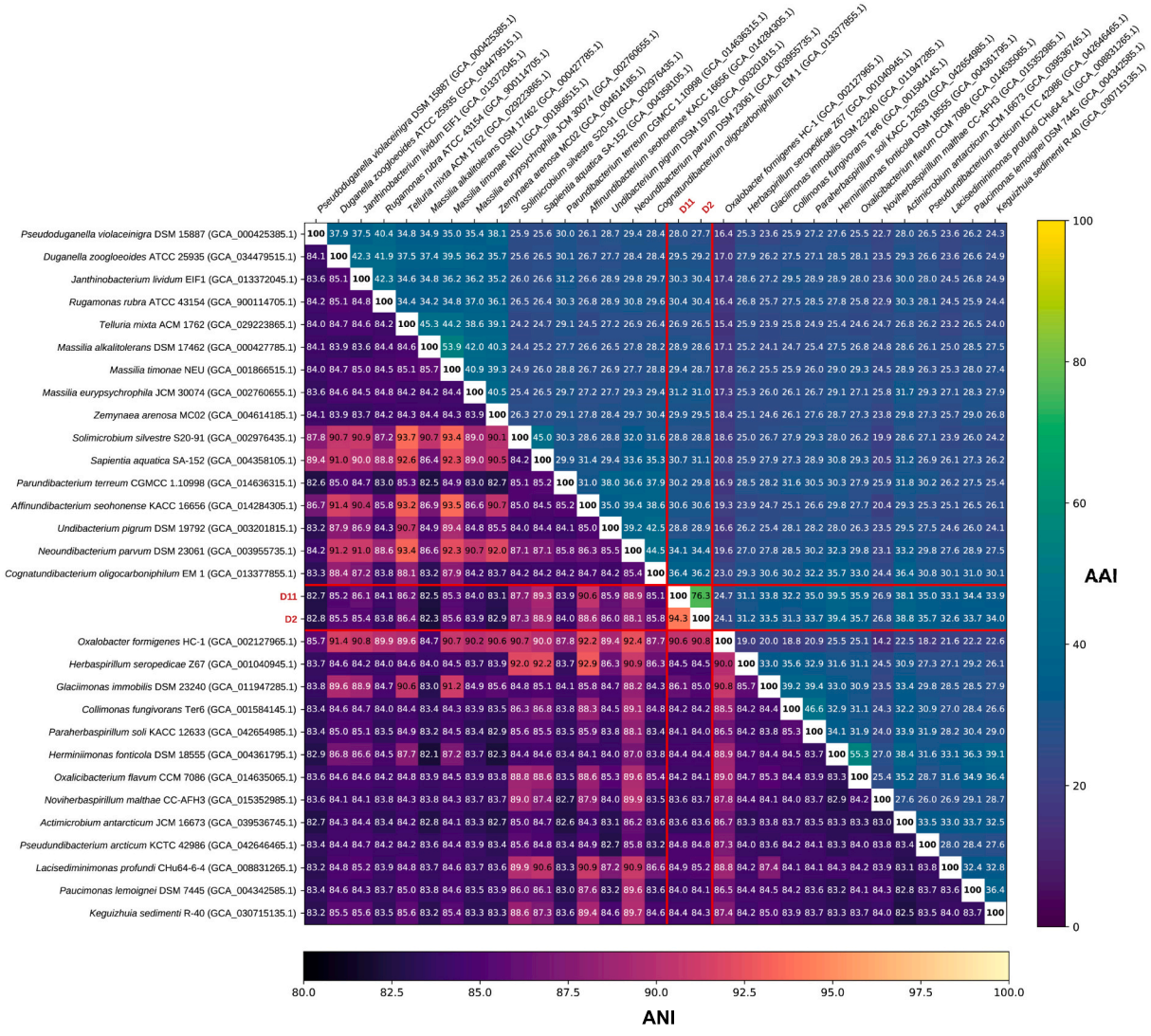

Fig. 3. Pairwise genome similarity among representatives of the family *Oxalobacteraceae*. Heatmaps show all-vs-all comparisons between genomes, with color intensity reflecting ANI (lower triangle) and AAI (upper triangle). The strains of *Gelidimonas* analyzed in this study are highlighted in red. (For interpretation of the references to color in this figure legend, the reader is referred to the web version of this article.)

levels.

Whole genome comparison using TYGS revealed the genomes most closely related to D2 and D11 are among members of the family *Oxalobacteraceae* (genera *Actimicrobium*, *Collimonas*, *Duganella*, *Herbaspirillum*, *Herminiimonas*, *Janthinobacterium*, *Massilia*, *Noviherbaspirillum*, *Oxalicibacterium*, *Paucimonas* and *Undibacterium*). However, in all cases the dDDH values (in relation to D2 and D11 genomes) were relatively low, below 15%.

The ANI values between D2 and D11 genomes and other members of the *Oxalobacteraceae* were similarly low, ranging from 82.7% to 90.8%, and the average amino acid identity (AAI) of their proteomes was below 39.5%, indicating the taxonomic distinctness of these strains (Fig. 3). Indeed, GTDB-Tk assigned the strains D11 and D2 to an unnamed genus with the placeholder name g_AVCC01, but not to any of the species-level taxa that are already defined. In Genome Taxonomy Database (GTDB) Release 10-RS226 (16th April 2025), this genus includes eight published genomes, all of which are metagenome-assembled genomes (MAGs) and six of which are derived from polar environments (Table S3).

A core genome phylogeny of the *Oxalobacteraceae* (Fig. 4 and Fig. S5) unambiguously placed the strains D2 and D11 within the *Oxalobacteraceae* but they were not closely related to any existing genus. Instead, they formed a well-supported clade together with the eight published MAGs assigned by GTDB to the genus g_AVCC01, which is clearly separated from all named genera. Therefore, we propose the establishment of a new genus, *Gelidimonas*. The name *Gelidimonas* is derived from the Latin *gelidus* (cold, icy) and the Greek *monas* (μονάς, unit, single-celled organism), referring to a bacterium associated with cold environments. Based on significant differences in metabolic properties and whole-genome comparisons, we propose to classify D2 and D11 as novel species within the genus *Gelidimonas*: *Gelidimonas diazotrophica* sp. nov. (D2), reflecting its ability to fix nitrogen, and *Gelidimonas denitrificans* sp. nov. (D11), highlighting its denitrification capacity.

The most closely related MAGs to D2 and D11 originated from glacier sediment in Iceland, and from a geothermal spring in northwest Spitsbergen, some 288 km north of the sample site for D11 and D2. There are also three related MAGs from a single site in Antarctica, while the remaining two genomes are from Canada and northern USA. Thus, there is a striking prevalence of samples from the Arctic or the Antarctic, so the genus name *Gelidimonas*, reflecting icy cold (gelid) environments, is apt.

Proteins specific to Gelidimonas

Of the 3625 predicted proteins of *Gelidimonas denitrificans* D11, 40 were present in all nine high-quality *Gelidimonas* genomes but absent in all 184 type strains of other species in the *Oxalobacteraceae* (Table S4). The tenth known *Gelidimonas* genome assembly, cluster3_bin.239, a seriously incomplete MAG, had 33 of the 40 proteins. While the functions of most of these proteins are not known, there is a group of six consecutive proteins (1287–1292) that are annotated as associated with formate hydrogenlyase. These proteins were not found in any genomes of isolates in the *Oxalobacteraceae* outside the genus *Gelidimonas*, although some were detected in a few MAGs. BLAST search revealed,

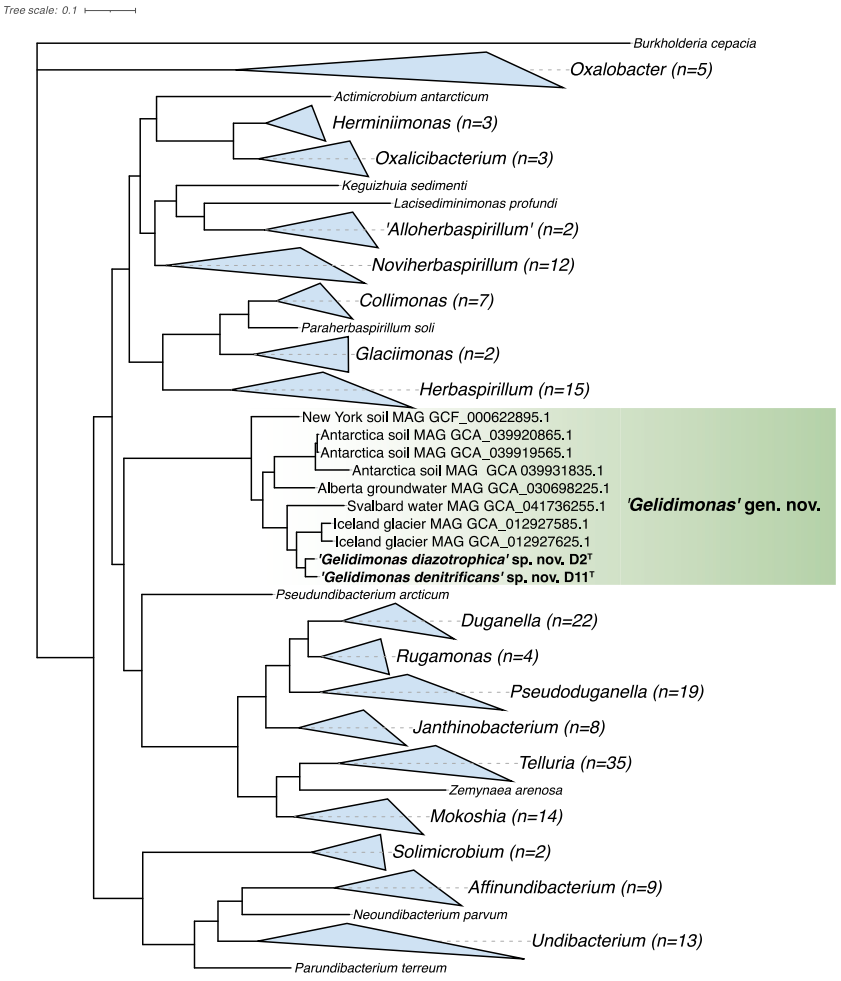

Fig. 4. The phylogenomic tree of the family *Oxalobacteraceae* based on the core family proteome (375 proteins). *Burkholderia cepacia* was used as an outgroup. The scale bar represents 0.1 substitutions per amino acid position.

though, that they were widespread in strains of some other *Betaproteobacteria*, such as *Paraburkholderia* spp.

Phylogenomic evidence for the new genus Gelidimonas

There are 29 validly published names of the genera in the family *Oxalobacteraceae*, and three recent studies have refined the taxonomy of this family. A phylogenomic study of the entire family, using consistent metrics for genus demarcation, proposed a number of new genera (Ma et al., 2023). Among other changes, the genus *Undibacterium* was subdivided, creating new genera *Affinundibacterium*, *Neoundibacterium* and *Parundibacterium* to accommodate divergent members. *Sapientia* was merged into *Solimicrobium*, some misplaced species of *Rugamonas* were moved to *Duganella* (though we have retained the name *Rugamonas* for the core clade) and *'Alloherbaspirillum'* (not yet validly published) was created to restore the monophyly of *Noviherbaspirillum*. All the proposed changes are well supported by genomic data. Another study reclassified all species of *Massilia* and *Naxibacter* into the genera *Telluria*, *Mokoshia* and *Zemynaea* on the basis of genomic and phenotypic data (Bowman, 2023). These new combinations are well supported and validly published. More recently, another study of *Undibacterium* has recognised that *U. arcticum* is distant from the rest of the genus and transferred it to a new genus *Pseudundibacterium*, and also split the main *Undibacterium* clade further with the creation of *Cognatundibacterium* (Lu et al., 2025). These three studies provide a more consistent basis for defining the genomic depth of individual genera within the *Oxalobacteraceae*, and we have used the new names in our phylogenetic analysis (with the exception of *Cognatundibacterium*, as this recent proposal is not directly relevant to our study).

The core genome phylogenetic analysis of the family performed in this study (Fig. 4 and Fig. S5) showed strong support for both the currently accepted genera and the genera proposed by Ma and colleagues and by Bowman (Ma et al., 2023; Bowman, 2023), as well as the newly proposed *Pseudundibacterium* (Lu et al., 2025). The analysis revealed that the two new isolates, D11 and D2, belong to the same novel genus, distantly related to other genera of *Oxalobacteraceae*. We propose to name the genus *Gelidimonas,* with D11 as the type strain of the type species *G. denitrificans* and D2 as the type strain of *G. diazotrophica*.

Distinguishing characteristics of the genus Gelidimonas

The comparative analysis of morphological, physiological, and molecular data for the proposed *Gelidimonas* species and the type strains of 29 genera within the family *Oxalobacteraceae* (Table S5) revealed that *Gelidimonas* is currently the only genus comprising exclusively psychrophilic strains. The two dominant fatty acids identified in both strains of the genus *Gelidimonas* (C16:1 ω7c and C16:0) are indicated as dominant in about half of the genera within the *Oxalobacteraceae* family and are therefore not useful characteristics for discriminating genera within the family (Table S5). At the same time, C18:1 ω9t appears to be specific to species *G. diazotrophica* (D2), as it has not been reported as a dominant fatty acid in any type species representing other genera of the *Oxalobacteraceae* family.

In addition to the experimentally determined properties, we identified 40 proteins that were characteristic of *Gelidimonas* but absent in other members of the *Oxalobacteraceae* (Table S4). We can expect that these confer genus-specific phenotypes, although the only function that can be identified with some certainty is provided by a group of six proteins (FKCLFG_01197 to FKCLFG_012020) that are constituents of formate hydrogenlyase. This enzyme complex includes formate dehydrogenase and hydrogenase and leads to the formation of molecular hydrogen (H_2) under oxic conditions (McDowall et al., 2014).

Protologues of *Gelidimonas* gen. nov., *G. diazotrophica* sp. nov. and *G. denitrificans* sp. nov. are presented in Table 3.

Table 3
Description of *Gelidimonas* gen. nov., *Gelidimonas diazotrophica* sp. nov. and *Gelidimonas denitrificans* sp. nov.

Guiding Code for Nomenclature	ICNP	ICNP	ICNP
Nature of the type material		Strain	Strain
Genus name	*Gelidimonas*		
Species name		*Gelidimonas diazotrophica*	*Gelidimonas denitrificans*
Genus status	gen. nov.		
Genus etymology	Ge.li.di.mo'nas. L. masc. adj. *gelidus*, cold; L. fem. n. *monas*, a unit, a monad; N.L. fem. n. *Gelidimonas*, a cold monad (referring to the cold environment where these bacteria have been isolated)		
Type species of the genus	*Gelidimonas denitrificans*		
Specific epithet		*diazotrophica*	*denitrificans*
Species status		sp. nov.	sp. nov.
Species etymology		di.a.zo.tro'phi.ca. Gr. adv. *dis*, twice, doubly; N.L. neut. n. *azotum*, nitrogen; N. L. pref. *diazo-*, pertaining to dinitrogen (in compound words); N.L. masc. adj. *trophicus*, nursing, tending; from Gr. masc. adj. *trophikos*; N.L. fem. adj. *diazotrophica*, growing on dinitrogen	de.ni.tri'fi.cans. N. L. v. *denitrifico*, to denitrify; N.L. fem. part. adj. *denitrificans*, denitrifying
Designation of the Type Strain		D2^T	D11^T
Strain Collection Numbers		DSM 120165^T = LMG 34059^T	DSM 120166^T = LMG 34060^T
Type Genome		GenBank = JBSYGK000000000	GenBank = JBSYGS000000000
Genome status		Complete	Complete
Genome size		3,855,409 bp	3,673,767 bp
GC mol%		55.3	55.4
16S rRNA gene accession no.		PX735051	PX735050
Description of the new taxon and diagnostic traits	Cells are Gram-negative, rod-shaped. Growth occurs in an aerobic and anaerobic atmosphere. Catalase-negative and oxidase-negative. The major cellular fatty acids are C16:1 ω7c and C16:0. Strains in this	Cells are Gram-negative, rod-shaped (approx. 1.8–2 μm long and 0.5 μm wide), motile, nonsporulating, oxidase and catalase negative. Colonies on R2A medium are circular, convex with entire edges, smooth, white coloured, of 0.5–1 mm in diameter.	Cells are Gram-negative, rod-shaped (approx. 2–3.2 μm long and 0.8 μm wide), motile, nonsporulating, oxidase and catalase negative. Colonies on R2A medium are circular, convex with entire edges, smooth, white coloured, of 0.3–1

(*continued on next page*)

Table 3 (*continued*)

Guiding Code for Nomenclature	ICNP	ICNP	ICNP
	genus typically have the genes to produce a set of proteins that are absent from other species in the family *Oxalobacteraceae* (Table S4). In particular, these include proteins of the formate hydrogenlyase complex, which is predicted to enable the release of molecular hydrogen under anaerobic conditions.	Growth is observed at 5-20 °C with an optimum at 10 °C, and a pH between 5.5 and 8.0, with an optimum of pH 6.0–6.5. NaCl is not required for growth, but cells can tolerate up to 3% (w/v) NaCl. Growth occurs in an aerobic and anaerobic atmosphere on Nutrient Agar and R2A. Growth not apparent on Luria Bertani and Trypticase Soya Broth. In the API ZYM, the strain is positive for: alkaline phosphatase, valine arylamidase, α-chymotripsin, leucine arylamidase, acid phosphatase, and naphthol-AS-BI-phosphohydrolase. In the API 20 NE, the strain is positive for: nitrate reduction, assimilation of malic acid, trisodium citrate and potassium gluconate. Plate test analysis performed using Biolog system GEN III indicated that strain has the ability to oxidize following carbon sources: Acetic Acid, Bromo-Succinic Acid, Citric Acid, D-Aspartic Acid, D-Malic Acid, L-Malic Acid, Propionic Acid, Sodium Lactate 1%, α-Keto-Butyric Acid, β-Hydroxy-D,L-Butyric Acid, γ-Amino-Butyric Acid and D-Serine. The sensitivity assay was negative for Rifamycin SV and Lincomycin. The major cellular fatty acids are C16:1 ω7c, C18:1 ω9t and C16:0. Ability to N_2 fixation and N_2O production was confirmed. PHA production was shown.	mm in diameter. Growth is observed at 5-15 °C with an optimum at 10 °C, and a pH between 5.5 and 8.0, with an optimum of pH 6.5–7.0. NaCl is not required for growth, but cells can tolerate up to 3% (w/v) NaCl. Growth occurs in an aerobic and anaerobic atmosphere on Luria-Bertani, Nutrient Agar, R2A and Trypticase Soya Broth. In the API ZYM, the strain is positive for: leucine arylamidase, acid phosphatase, and naphthol-AS-BI-phosphohydrolase. In the API 20 NE, the strain is positive for: nitrate reduction, assimilation of malic acid, production of indole and esculin hydrolysis. Plate test analysis performed using Biolog system GEN III indicated that strain has the ability to oxidize following carbon sources: Acetic Acid, Citric Acid, D-Malic Acid, L-Malic Acid, Propionic Acid, Sodium Lactate 1%, α-Keto-Butyric Acid, β-Hydroxy-D,L-Butyric Acid and γ-Amino-Butyric Acid. The sensitivity assay was negative for lincomycin. The major cellular fatty acids are C16:1 ω7c and C16:0. Ability to N_2O production was confirmed. PHA production was shown.

Table 3 (*continued*)

Guiding Code for Nomenclature	ICNP	ICNP	ICNP
Country of origin		Norway	Norway
Region of origin		Spitsbergen, Svalbard	Spitsbergen, Svalbard
Date of isolation		10/10/2021	10/10/2021
Source of isolation		Ornithogenic soil	Ornithogenic soil
Sampling date		30/08/2021	30/08/2021
Latitude		77°00′33.3″N	77°00′33.3″N
Longitude		15°31′49.1″E	15°31′49.1″E
Number of strains in study		1	1
Information related to the Nagoya Protocol		–	–

Metagenomic analysis of D2- and D11-related strains in Arctic ornithogenic soil

To assess the presence and abundance of D2- and D11-related strains in their natural environment, we performed metagenomic analyses. Metagenomic DNA was extracted directly from the soil sample (OS – ornithogenic soil) from which the D2 and D11 strains were originally isolated, and from soil incubated for 100 days under anaerobic conditions on R2A medium supplemented with nitrates to enrich for denitrifiers (ORP). The sequencing generated high-quality data (available in the Sequence Read Archive, SRA, database under accession numbers SRR37098257 for the OS metagenome and SRR37098256 for the ORP metagenome), with over 86% of bases exhibiting a Phred Score above Q30, and yielded an average of 96–115 MR/sample.

Mapping of metagenomic reads obtained revealed that genomic sequences of both strains were present in these datasets (Fig. 5). Reads from the OS metagenome covered 71% (D2) and 61% (D11) of the genome, while those from the ORP metagenome covered 91% (D2) and 86% (D11). The mapped reads represented 0.63% and 0.71% of the relative abundance in the raw (OS) metagenome and 1.19% and 1.25% in the enriched (ORP) culture-originating metagenome, respectively.

The mean genome coverage depth was 13× and 15× in the OS metagenome and 37× and 38× in the ORP metagenome, with local maxima of approximately 1050× and 1450×. In conclusion, bacteria closely related to D2 and D11 appear to be active members of the ornithogenic soil microbiome, with their higher abundance and genome coverage in enriched metagenomes suggesting a key role in denitrification under natural conditions.

Conclusion

The strains analyzed in this study, D2 and D11, despite exhibiting striking genome synteny and sequence conservation, display distinct metabolic properties. Strain D2 harbors several unique gene clusters associated with a chemolithoautotrophic lifestyle as well as N_2 assimilation, likely acquired horizontally from other members of the family *Oxalobacteraceae.* Detailed phylogenomic analysis revealed that the strains D2 and D11 represent two distinct but closely related species. We propose classifying them into a novel genus *Gelidimonas*, with the species designated as *Gelidimonas diazotrophica* sp. nov. (D2) and *Gelidimonas denitrificans* sp. nov. (D11). This work provides guidelines for the correct identification and classification of further isolates of bacteria from the family *Oxalobacteraceae*.

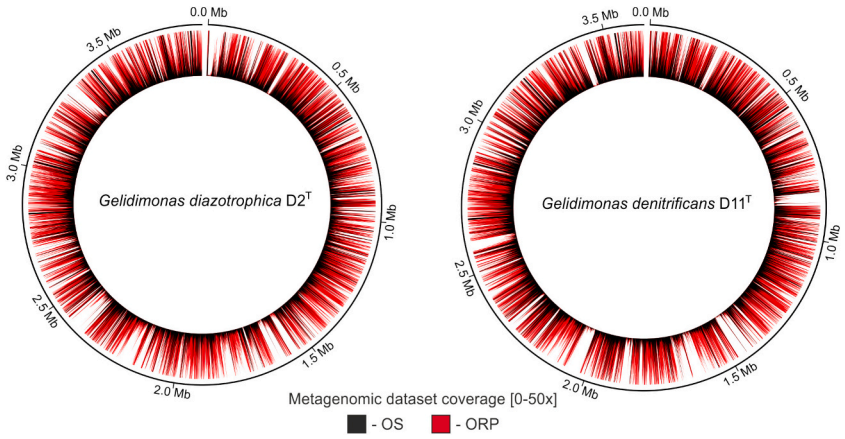

Fig. 5. Distribution of metagenomic read coverage across the D2 and D11 genomes. OS refers to the ornithogenic soil metagenome (soil samples from which the D2 and D11 strains originated), whereas ORP denotes the same ornithogenic soil metagenome enriched in denitrifying bacteria following incubation on R3A medium supplemented with nitrates. The inner track shows metagenomic read coverage calculated using a 500-bp sliding window. Coverage values were capped at 50× to maintain visual clarity and highlight local coverage gaps. Maximum coverage values were as follows: D2 – OS: 1014×, ORP: 1432×; D11 – OS: 1075×, ORP: 1475 ×.

CRediT authorship contribution statement

Jakub Grzesiak: Writing – review & editing, Investigation, Data curation, Conceptualization. **Julia Brzykcy:** Writing – review & editing, Resources, Investigation, Funding acquisition. **Peter Young:** Writing – review & editing, Writing – original draft, Investigation, Data curation, Conceptualization. **Elvira Krakowska:** Writing – review & editing, Validation, Investigation. **Robert Stasiuk:** Writing – review & editing, Methodology, Investigation. **Kamil Krakowski:** Writing – review & editing, Writing – original draft, Visualization, Investigation, Data curation. **Przemysław Decewicz:** Writing – review & editing, Visualization, Investigation, Data curation. **Alina Kiedryńska:** Writing – review & editing, Investigation. **Renata Matlakowska:** Writing – review & editing, Writing – original draft, Visualization, Supervision, Project administration, Investigation, Funding acquisition, Data curation, Conceptualization. **Dariusz Bartosik:** Writing – review & editing, Writing – original draft, Supervision, Investigation, Data curation, Conceptualization.

Funding

This work was in part supported by the program of the Ministry of Science and Higher Education (Poland) – Excellence Initiative – Research University (2020–2026), grant no.: BOB-IDUB-622-858/2023; Priority Research Areas – Science for the Planet and the Polar Mission 2021, Edu Arctic (Institute of Geophysics Polish Academy of Sciences).

Declaration of competing interest

The authors declare that they have no known competing financial interests or personal relationships that could have appeared to influence the work reported in this paper.

Acknowledgements

We thank Tengfei Ma for sharing the sequences of the core proteins of the *Oxalobacteraceae*. Metagonomic sequencing was performed thanks to Genomics Core Facility CeNT UW (RRID:SCR_022718), using NovaSeq 6000 platform.

Appendix A. Supplementary data

Supplementary data to this article can be found online at https://doi.org/10.1016/j.syapm.2026.126730.

Data availability

The Whole Genome Shotgun projects of *G. diazotrophica* and *G. denitrificans* have been deposited at DDBJ/ENA/GenBank under the accession numbers JBSYGK000000000 and JBSYGS000000000, respectively. The versions described in this paper are version JBSYGK010000000 and JBSYGS010000000, respectively

References

Allison, M.J., Dawson, K.A., Mayberry, W.R., Foss, J.G., 1985. *Oxalobacter formigenes* gen. nov., sp. nov.: oxalate-degrading anaerobes that inhabit the gastrointestinal tract. Arch. Microbiol. 141, 1–7. https://doi.org/10.1007/BF00446731.

Altschul, S.F., Madden, T.L., Schäffer, A.A., Zhang, J., Zhang, Z., Miller, W., Lipman, D.J., 1997. Gapped BLAST and PSI-BLAST: a new generation of protein database search programs. Nucleic Acids Res. 25, 3389–3402. https://doi.org/10.1093/nar/25.17.3389.

Aragno, M., Schlegel, H.G., 1992. The hydrogen-oxidizing bacteria. In: Starr, M.P., Stolp, H., Trüper, H.G., Balows, A., Schlegel, H.G. (Eds.), The Prokaryotes, 2nd ed. 1. Springer-Verlag, Berlin Heidelberg, p. 865.

Aroney, S.T.N., Newell, R.J.P., Nissen, J.N., Camargo, A.P., Tyson, G.W., Woodcroft, B.J., 2025. CoverM: read alignment statistics for metagenomics. Bioinformatics 41, btaf147. https://doi.org/10.1093/bioinformatics/btaf147.

Atlas, R.M., 2010. Handbook of Microbiological Media, 4th ed. CRC Press, Boca Raton.

Auch, A.F., von Jan, M., Klenk, H.P., Göker, M., 2010. Digital DNA-DNA hybridization for microbial species delineation by means of genome-to-genome sequence comparison. Stand. Genomic Sci. 2, 117–134. https://doi.org/10.4056/sigs.531120.

Baldani, J.I., Rouws, L., Cruz, L.M., Olivares, F.L., Schmid, M., Hartmann, A., 2014. The family *Oxalobacteraceae*. In: Rosenberg, E., DeLong, E.F., Lory, S., Stackebrandt, E., Thompson, F. (Eds.), The Prokaryotes. Springer, Berlin, Heidelberg. https://doi.org/10.1007/978-3-642-30197-1_291.

Bonenfant, Q., Noé, L., Touzet, H., 2022. Porechop_ABI: discovering unknown adapters in ONT sequencing reads for downstream trimming. https://doi.org/10.1101/2022.07.07.499093.

Bonfield, J.K., Marshall, J., Danecek, P., Li, H., Ohan, V., Whitwham, A., Keane, T., Davies, R.M., 2021. HTSlib: C library for reading/writing high-throughput sequencing data. Gigascience 10, giab007. https://doi.org/10.1093/gigascience/giab007.

Bouras, G., Grigson, S.R., Papudeshi, B., Mallawaarachchi, V., Roach, M.J., 2024. Dnaapler: a tool to reorient circular microbial genomes. J. Open Source Softw. 9, 5968. https://doi.org/10.21105/joss.05968.

Bowman, J.P., 2023. Genome-wide and constrained ordination-based analyses of EC code data support reclassification of the species of *Massilia* La Scola et al. 2000 into *Telluria* Bowman et al. 1993, *Mokoshia* gen. nov. and *Zemynaea* gen. nov. Int. J. Syst. Evol. Microbiol. 73, 005991. https://doi.org/10.1099/ijsem.0.005991.

Brzykcy, J., Matlakowska, R., Grzesiak, J., 2026. Evaluation of high Arctic terrestrial habitats as potential hotspots of nitrous oxide emissions (Hornsund region, South Spitsbergen). bioRxiv. https://doi.org/10.64898/2026.02.27.708492.

Chalita, M., Kim, Y.O., Park, S., Oh, H.S., Cho, J.H., Moon, J., Baek, N., Moon, C., Lee, K., Yang, J., Nam, G.G., Jung, Y., Na, S.I., Bailey, M.J., Chun, J., 2024. EzBioCloud: a genome-driven database and platform for microbiome identification and discovery. Int. J. Syst. Evol. Microbiol. 74, 006421. https://doi.org/10.1099/ijsem.0.006421.

Chen, S., 2023. Ultrafast one-pass FASTQ data preprocessing, quality control, and deduplication using fastp. iMeta 2, e107. https://doi.org/10.1002/imt2.107.

Chen, S., Zhou, Y., Chen, Y., Gu, J., 2018. Fastp: an ultra-fast all-in-one FASTQ preprocessor. Bioinformatics 34, i884–i890. https://doi.org/10.1093/bioinformatics/bty560.

Clark, D.P., Cronan, J.E., 2005. Two-carbon compounds and fatty acids as carbon sources. EcoSal Plus 1 (2). https://doi.org/10.1128/ecosalplus.3.4.4.

Couvin, D., Bernheim, A., Toffano Nioche, C., Touchon, M., Michalik, J., Néron, B., Rocha, E.P.C., Vergnaud, G., Gautheret, D., Pourcel, C., 2018. CRISPRCasFinder, an update of CRISRFinder, includes a portable version, enhanced performance and integrates search for Cas proteins. Nucleic Acids Res. 46 (W1), W246–W251. https://doi.org/10.1093/nar/gky425.

Danecek, P., Bonfield, J.K., Liddle, J., Marshall, J., Ohan, V., Pollardm, M.O., Whitwhamn, A., Keane, T., McCarthy, S.A., Davies, R.M., Li, H., 2021. Twelve years of SAMtools and BCFtools. Gigascience 10, giab008. https://doi.org/10.1093/gigascience/giab008.

Descamps, S., Aars, J., Fuglei, E., Kovacs, K.M., Lydersen, C., Pavlova, O., Pedersen, Å.Ø., Ravolainen, V., Strøm, H., 2017. Climate change impacts on wildlife in a high Arctic archipelago – Svalbard, Norway. Glob. Chang. Biol. https://doi.org/10.1111/gcb.13381.

Edgren, T., Nordlund, S., 2004. The fixABCX genes in *Rhodospirillum rubrum* encode a putative membrane complex participating in electron transfer to nitrogenase. J. Bacteriol. 186, 2052–2060. https://doi.org/10.1128/JB.186.7.2052-2060.2004.

Elliott, M.L., Des Jardin, E.A., 1999. Comparison of media and diluents for enumeration of aerobic bacteria from Bermuda grass golf course putting greens. J. Microbiol. Methods 34, 193–202. https://doi.org/10.1016/S0167-7012(98)00088-8.

Ernakovich, J.G., Barbato, R.A., Rich, V.I., Schädel, C., Hewitt, R.E., Doherty, S.J., Whalen, E.D., Abbott, B.W., Barta, J., Biasi, C., Chabot, C.L., Hultman, J., Knoblauch, C., Vetter, M.C.Y.L., Leewis, M.C., Liebner, S., Mackelprang, R., Onstott, T.C., Richter, A., Schütte, U.M.E., Siljanen, H.M.P., Taş, N., Timling, I., Vishnivetskaya, T.A., Waldrop, M.P., Winkel, M., 2022. Microbiome assembly in thawing permafrost and its feedbacks to climate. Glob. Chang. Biol. 28, 5007–5026. https://doi.org/10.1111/gcb.16231.

Floyd, K.A., Lee, C.K., Xian, W., Nametalla, M., Valentine, A., Crair, B., Zhu, S., Hughes, H.Q., Chlebek, J.L., Wu, D.C., Park, J.H., Farhat, A.M., Lomba, C.J., Ellison, C.K., Brun, Y.V., Campos-Gomez, J., Dalia, A.B., Liu, J., Biais, N., Wong, G.C. L., Yildiz, F.H., 2020. C-di-GMP modulates type IV MSHA pilus retraction and surface attachment in *vibrio cholerae*. Nat. Commun. 11, 1549. https://doi.org/10.1038/s41467-020-15331-8.

Grant, J.R., Enns, E., Marinier, E., Mandal, A., Herman, E.K., Chen, C.-Y., Graham, M., Van Domselaar, G., Stothard, P., 2023. Proksee: in depth characterization and visualization of bacterial genomes. Nucleic Acids Res. 51 (W1), W484–W492. https://doi.org/10.1093/nar/gkad326.

Greening, C., Biswas, A., Carere, C., Jackson, C.J., Taylor, M.C., Stott, M.B., Cook, G.M., 2016. Genomic and metagenomic surveys of hydrogenase distribution indicate H_2 is a widely utilised energy source for microbial growth and survival. ISME J. 10, 761–777. https://doi.org/10.1038/ismej.2015.153.

Grzesiak, J., Kaczyńska, A., Gawor, J., Żuchniewicz, K., Aleksandrzak-Piekarczyk, T., Gromadka, R., Zdanowski, M.K., 2020. A smelly business: microbiology of Adélie penguin guano (point Thomas rookery, Antarctica). Sci. Total Environ. 714, 136714. https://doi.org/10.1016/j.scitotenv.2020.136714.

Hackmann, T.J., 2025. Setting new boundaries of 16S rRNA gene identity for prokaryotic taxonomy. Int. J. Syst. Evol. Microbiol. 75, 006747. https://doi.org/10.1099/ijsem.0.006747.

Hazelbauer, G.L., Falke, J.J., Parkinson, J.S., 2008. Bacterial chemoreceptors: high-performance signaling in networked arrays. Trends Biochem. Sci. 33, 9–19. https://doi.org/10.1016/j.tibs.2007.09.014.

Hunter, J.D., 2007. Matplotlib: a 2D graphics environment. Comput. Sci. Eng. 9, 90–95. https://doi.org/10.1109/MCSE.2007.55.

Jones, C.M., Stres, B., Rosenquist, M., Hallin, S., 2008. Phylogenetic analysis of nitrite, nitric oxide, and nitrous oxide respiratory enzymes reveal a complex evolutionary history for denitrification. Mol. Biol. Evol. 25, 1955–1966. https://doi.org/10.1093/molbev/msn146.

Kadowaki, M.A., Müller-Santos, M., Rego, F.G., Souza, E.M., Yates, M.G., Monteiro, R.A., Pedrosa, F.O., Chubatsu, L.S., Steffens, M.B., 2011. Identification and characterization of PhbF: a DNA binding protein with regulatory role in the PHB metabolism of *Herbaspirillum seropedicae* SmR1. BMC Microbiol. 11, 230. https://doi.org/10.1186/1471-2180-11-230.

Kalyaanamoorthy, S., Minh, B.Q., Wong, T.K.F., von Haeseler, A., Jermiin, L.S., 2017. ModelFinder: fast model selection for accurate phylogenetic estimates. Nat. Methods 14, 587–589. https://doi.org/10.1038/nmeth.4285.

Kim, D., Park, S., Chun, J., 2021. Introducing EzAAI: a pipeline for high throughput calculations of prokaryotic average amino acid identity. J. Microbiol. 59, 476–480. https://doi.org/10.1007/s12275-021-1154-0.

Kolmogorov, M., Yuan, J., Lin, Y., Pevzner, P.A., 2019. Assembly of long, error-prone reads using repeat graphs. Nat. Biotechnol. 37, 540–546. https://doi.org/10.1038/s41587-019-0072-8.

Korsak, D., Szuplewska, M., Kozłowska, P., Krakowski, K., Chmielowska, C., Wawrzyniak, P., Maćkiw, E., Bartosik, D., 2025. Characterization of *Cronobacter* spp. isolated from food products in Poland and comparative genomic analysis of *Cronobacter sakazakii* isolate MK_10 and a clinical strain associated with a fatal neonatal infection. Front. Microbiol. 16, 1713963. https://doi.org/10.3389/fmicb.2025.1713963.

Kuczyńska-Wiśnik, D., Stojowska-Swędrzyńska, K., Laskowska, E., 2024. Intracellular protective functions and therapeutical potential of trehalose. Molecules 29, 2088. https://doi.org/10.3390/molecules29092088.

Kuzmanović, N., Fagorzi, C., Mengoni, A., Lassalle, F., diCenzo, G.C., 2021. Taxonomy of *Rhizobiaceae* revisited: proposal of a new framework for genus delimitation. Int. J. Syst. Evol. Microbiol. 72, 005243. https://doi.org/10.1099/ijsem.0.005243.

Li, H., Handsaker, B., Wysoker, A., Fennell, T., Ruan, J., Homer, N., Marth, G., Abecasis, G., Durbin, R., 2009. 1000 genome project data processing subgroup. The sequence alignment/map format and SAMtools. Bioinformatics 25, 2078–2079. https://doi.org/10.1093/bioinformatics/btp352.

Lu, H.-B., Kong, L.-Y., Chen, L., Chen, G.-J., Wang, J.-J., 2025. Isolation of diverse *Undibacterium*-related strains from alpine lakes and re-examining the taxonomic status of this genus. Syst. Appl. Microbiol. 48 (6), 126661. https://doi.org/10.1016/j.syapm.2025.126661.

Lunau, M., Lemke, A., Walther, K., Martens-Habbena, W., Simon, M., 2005. An improved method for counting bacteria from sediments and turbid environments by epifluorescence microscopy. Environ. Microbiol. 7, 961–968. https://doi.org/10.1111/j.1462-2920.2005.00767.x.

Ma, T., Xue, H., Piao, C., Jiang, N., Li, Y., 2023. Genome-based analyses of family Oxalobacteraceae reveal the taxonomic classification. Res. Microbiol. 174, 104076. https://doi.org/10.1016/j.resmic.2023.104076.

Malard, L.A., Pearce, D.A., 2018. Microbial diversity and biogeography in Arctic soils. Environ. Microbiol. Rep. 10, 611–625. https://doi.org/10.1111/1758-2229.12680.

Manni, M., Berkeley, M.R., Seppey, M., Simão, F.A., Zdobnov, E.M., 2021. BUSCO update: novel and streamlined workflows along with broader and deeper phylogenetic coverage for scoring of eukaryotic, prokaryotic, and viral genomes. Mol. Biol. Evol. 38, 4647–4654. https://doi.org/10.1093/molbev/msab199.

McDowall, J.S., Murphy, B.J., Haumann, M., Palmer, T., Armstrong, F.A., Sargent, F., 2014. Bacterial formate hydrogenlyase complex. Proc. Natl. Acad. Sci. USA 111, E3948–E3956. https://doi.org/10.1073/pnas.1407927111.

McKinney, W., 2010. Data structures for statistical computing in Python. In proceedings of the 9th Python in science conference, pp. 56–61. https://doi.org/10.25080/Majora-92bf1922-00.

Medema, M.H., Blin, K., Cimermancic, P., de Jager, V., Zakrzewski, P., Fischbach, M.A., Weber, T., Takano, E., Breitling, R., 2011. antiSMASH: rapid identification, annotation and analysis of secondary metabolite biosynthesis gene clusters in bacterial and fungal genome sequences. Nucleic Acids Res. 39, W339–W346. https://doi.org/10.1093/nar/gkr466.

Meier-Kolthoff, J.P., Göker, M., 2019. TYGS is an automated high-throughput platform for state-of-the-art genome based taxonomy. Nat. Commun. 10, 2182. https://doi.org/10.1038/s41467-019-10210-3.

Meloni, M., Gurrieri, L., Fermani, S., Velie, L., Sparla, F., Crozet, P., Henri, J., Zaffagnini, M., 2023. Ribulose-1,5-bisphosphate regeneration in the Calvin-Benson-Bassham cycle: focus on the last three enzymatic steps that allow the formation of Rubisco substrate. Front. Plant Sci. 14. https://doi.org/10.3389/fpls.2023.1130430.

Minh, B.Q., Schmidt, H.A., Chernomor, O., Schrempf, D., Woodhams, M.D., von Haeseler, A., Lanfear, R., 2020. IQ-TREE 2: new models and efficient methods for phylogenetic inference in the genomic era. Mol. Biol. Evol. 37, 1530–1534. https://doi.org/10.1093/molbev/msaa015.

Mosier, A.R., 1998. Soil processes and global change. Biol. Fertil. Soils 27, 221–229.

Nanopore Technologies, 2025. Medaka. https://github.com/nanoporetech/medaka.

Ng, H.S., Wan, P.-K., Kondo, A., Chang, J.-S., Lan, J.C.-W., 2023. Production and recovery of ectoine: a review of current state and future prospects. Processes 11, 339. https://doi.org/10.3390/pr11020339.

Nie, L., Xiao, Y., Zhou, T., Feng, H., He, M., Liang, Q., Mu, K., Nie, H., Huang, Q., Chen, W., 2024. Cyclic di-GMP inhibits nitrate assimilation by impairing the antitermination function of NasT in *Pseudomonas putida*. Nucleic Acids Res. 52, 186–203. https://doi.org/10.1093/nar/gkad1117.

Pan, Y.-T., Carroll, J.D., Asano, N., Pastuszak, I., Edavana, V.K., Elbein, A.D., 2008. Trehalose synthase converts glycogen to trehalose. FEBS J. 275, 3408–3420. https://doi.org/10.1111/j.1742-4658.2008.06491.x.

Parks, D.H., Chuvochina, M., Chaumeil, P.A. Rinke, Mussig, A.J., Hugenholtz, P., 2020. A complete domain-to-species taxonomy for Bacteria and Archaea. Nat. Biotechnol. 38, 1079–1086. https://doi.org/10.1038/s41587-020-0501-8.

Pedrosa, F.O., Monteiro, R.A., Wassem, R., Cruz, L.M., Ayub, R.A., Colauto, N.B., Fernandez, M.A., Fungaro, M.H., Grisard, E.C., Hungria, M., et al., 2011. Genome of *Herbaspirillum seropedicae* strain SmR1, a specialized diazotrophic endophyte of tropical grasses. PLoS Genet. 7, e1002064. https://doi.org/10.1371/journal.pgen.1002064.

Pritchard, L., Glover, R.H., Humphris, S., Elphinstone, J.G., Toth, I.K., 2016. Genomics and taxonomy in diagnostics for food security: soft-rotting enterobacterial plant pathogens. Anal. Methods 8, 12–24. https://doi.org/10.1039/C5AY02550H.

Rao, N.N., Gómez-García, M.R., Kornberg, A., 2009. Inorganic polyphosphate: essential for growth and survival. Annu. Rev. Biochem. 78, 605–647. https://doi.org/10.1146/annurev.biochem.77.083007.093039.

Richter, M., Rosselló-Móra, R., Glöckner, F.O., Peplies, J., 2015. JSpeciesWS: a web server for prokaryotic species circumscription based on pairwise genome comparison. Bioinformatics 32, 929. doi:10.1093/bioinformatics/btv681.

Sasser, M., 2006. Bacterial identification by gas chromatographic analysis of fatty acids methyl esters (GC-FAME). MIDI Technical Note #101.

Schuur, E.A.G., Abbott, B.W., Commane, R., Ernakovich, J., Euskirchen, E., Hugelius, G., Grosse, G., Jones, M., Koven, C., Leshyk, V., Lawrence, D., Loranty, M.M., Mauritz, M., Olefeldt, D., Natali, S., Rodenhizer, H., Salmon, V., Schädel, C., Strauss, J., Treat, C., Turetsky, M., 2022. Permafrost and climate change: carbon cycle feedbacks from the warming Arctic. Annu. Rev. Environ. Resour. 47, 343–371. https://doi.org/10.1146/annurev-environ-012220-011847.

Schwengers, O., Jelonek, L., Dieckmann, M.A., Beyvers, S., Blom, J., Goesmann, A., 2021. Bakta: rapid and standardized annotation of bacterial genomes via alignment-

free sequence identification. Microb. Genomics 7, 000685. https://doi.org/10.1099/mgen.0.000685.
Sievers, F., Wilm, A., Dineen, D., Gibson, T.J., Karplus, K., Li, W., Lopez, R., McWilliam, H., Remmert, M., Söding, J., Thompson, J.D., Higgins, D.G., 2011. Fast, scalable generation of high-quality protein multiple sequence alignments using Clustal omega. Mol. Syst. Biol. 7, 539. https://doi.org/10.1038/msb.2011.75.
Siguier, P., Perochon, J., Lestrade, L., Mahillon, J., Chandler, M., 2006. ISfinder: the reference centre for bacterial insertion sequences. Nucleic Acids Res. 34 (Database issue), D32–D36. https://doi.org/10.1093/nar/gkj014.
Söding, J., Biegert, A., Lupas, A.N., 2005. The HHpred interactive server for protein homology detection and structure prediction. Nucleic Acids Res. 33 (Web Server issue), W244–W248. https://doi.org/10.1093/nar/gki408.
Stackebrandt, E., Ebers, J., 2006. Taxonomic parameters revisited: tarnished gold standards. Microbiol. Today 33, 152–155.
Vaser, R., Šikić, M., 2021. Time- and memory-efficient genome assembly with raven. Nat. Comput. Sci. 1, 332–336. https://doi.org/10.1038/s43588-021-00073-4.
Vasimuddin, M., Misra, S., Li, H., Aluru, S., 2019. Efficient architecture-aware acceleration of BWA-MEM for multicore systems. In: 2019 IEEE international parallel and distributed processing symposium (IPDPS), pp. 314–324. https://doi.org/10.1109/IPDPS.2019.00041.
Virtanen, P., Gommers, R., Oliphant, T.E., Haberland, M., Reddy, T., Cournapeau, D., Burovski, E., Peterson, P., Weckesser, W., Bright, J., van der Walt, S.J., Brett, M., Wilson, J., Millman, K.J., Mayorov, N., Nelson, A.R.J., Jones, E., Kern, R., Larson, E., Carey, C.J., Polat, I., Feng, Y., Moore, E.W., VanderPlas, J., Laxalde, D., Perktold, J., Cimrman, R., Henriksen, I., Quintero, E.A., Harris, C.R., Archibald, A.M., Ribeiro, A. H., Pedregosa, F., van Mulbregt, P., 2020. SciPy 1.0 contributors (2020). SciPy 1.0: fundamental algorithms for scientific computing in Python. Nat. Methods 17, 261–272. https://doi.org/10.1038/s41592-019-0686-2.
Walker, B.J., Abeel, T., Shea, T., Priest, M., Abouelliel, A., Sakthikumar, S., Cuomo, C.A., Zeng, Q., Wortman, J., Young, S.K., Earl, A.M., 2014. Pilon: an integrated tool for comprehensive microbial variant detection and genome assembly improvement. PLoS One 9, e112963. https://doi.org/10.1371/journal.pone.0112963.
Wang, M., Liu, G., Liu, M., Tai, C., Deng, Z., Song, J., Ou, H.-Y., 2024. ICEberg 3.0: functional categorization and analysis of the integrative and conjugative elements in bacteria. Nucleic Acids Res. 52 (D1), D732–D737. https://doi.org/10.1093/nar/gkad935.
Wick, R.R., Holt, K.E., 2021. Benchmarking of long-read assemblers for prokaryote whole genome sequencing. F1000Res. https://doi.org/10.12688/f1000research.21782.4.
Wick, R.R., Holt, K.E., 2022. Polypolish: short-read polishing of long-read bacterial genome assemblies. PLoS Comput. Biol. 18, e1009802. https://doi.org/10.1371/journal.pcbi.1009802.
Wick, R.R., Judd, L.M., Cerdeira, L.T., Hawkey, J., Méric, G., Vezina, B., Wyres, K.L., Holt, K.E., 2021. Trycycler: consensus long-read assemblies for bacterial genomes. Genome Biol. 22, 266. https://doi.org/10.1186/s13059-021-02483-z.
Wishart, D.S., Han, S., Saha, S., Oler, E., Peters, H., Grant, J.R., Stothard, P., Gautam, V., 2023. PHASTEST: faster than PHASTER, better than PHAST. Nucleic Acids Res. 51 (W1), W443–W450. https://doi.org/10.1093/nar/gkad382.
Yarza, P., Yilmaz, P., Pruesse, E., Glöckner, F.O., Ludwig, W., Schleifer, K.-H., Whitman, W.B., Euzéby, J., Amann, R., Rosselló-Móra, R., 2014. Uniting the classification of cultured and uncultured bacteria and archaea using 16S rRNA gene sequences. Nat. Rev. Microbiol. 12, 635–645. https://doi.org/10.1038/nrmicro3330.
Zumft, W.G., 1997. Cell biology and molecular basis of denitrification. Microbiol. Mol. Biol. Rev. 61, 533–616. https://doi.org/10.1128/mmbr.61.4.533-616.1997.